Preprint of paper published as Nucl. Instr. Meth. Phys. Res. B 267 (2009) 1235.

Amorphization of Ge nanocrystals embedded in amorphous silica under ion irradiation

Flyura Djurabekova [a,*], Marie Backman [a], Olli H. Pakarinen [a], Kai Nordlund [a], Leandro Araujo [b] and Mark Ridgway [b]

[a] *Helsinki Institute of Physics and Department of Physics, P.O. Box 43, FI-00014 University of Helsinki, Finland*

[b] *Department of Electronic Materials Engineering, Research School of Physical Sciences and Engineering, Australian National University, Canberra, ACT 0200, Australia*

Abstract

One of the key reasons why nanoscale materials behave differently from their bulk counterparts is that a large fraction of atoms reside at surfaces or interfaces. For instance, the melting point, hardness and even crystal structure of a nanocrystal can be dramatically different from that of the same element or compound in its conventional phase. Of particular interest from an ion beam modification point of view is how much the structural transformations induced by energetic ions in nanocrystals differ from those in the bulk phase. Using a combination of molecular dynamics (MD) computer simulations and *EXAFS* (Extended X-Ray Absorption Fine Structure) experiments, we show that the crystalline-to-amorphous transition in Ge nanocrystals occurs at a dose which is significantly (more than an order of magnitude) lower than that in the bulk phase. The MD simulations indicate that this is related to the outermost part of a structured nanocrystal being subjected to

an additional stress delivered by the amorphous surroundings. These results show that conventional models based on irradiation of bulk materials can not be used to estimate the susceptibility of nanocrystals to phase transitions.

Key words: Molecular dynamics simulation; Germanium; Nanocrystal; Silica; Interface; Ion irradiation

PACS: 78.55.Qr, 78.67.Bt, 79.60.Jv

1 Introduction

Modification of semiconductor crystal materials by high dose ion-beam irradiation is often hindered by their amorphization. Thus, the introduction of dopants into semiconductors renders them amorphous, which requires an extra annealing step for the recrystallization of irradiated materials [1]. At the same time, the preamorphization of Ge surface layers has been shown to have a positive effect allowing shallower layers of boron dopants [2,3]. This is why knowledge of the threshold doses which crystal structure can tolerate before collapsing into amorphous (amorphization dose) remain of high importance for the conventional microelectronic industry.

The existence of finite-size effects requires an additional thorough insight for the proper definition of amorphization dose for semiconductor nanocrystals embedded into amorphous matrices. In previous studies, it has been shown that the properties of nanocrystals may significantly vary from the properties of the same crystals in the bulk phase. For instance, the melting point of

* Corresponding author.
Email address: flyura.djurabekova@helsinki.fi (Flyura Djurabekova).

crystal structure of the nanosize can be significantly higher or lower than that of the same element or compound in its conventional phase depending on the nature of surrounding matter [4,5,6,7,8,9,10,11]. High-dose ion irradiation of elemental metal nanoclusters leads to the amorphization of their crystal structure, while it is known that elemental bulk metals can not be amorphized [12].

The semiconductor nanocrystals embedded into dielectric matrices have recently received an elevated interest due to the various potential applications in nanotechnology (see, for example, [13]). The fabrication process of such structures includes the irradiation by high energy (MeV range) ions during the inverse Ostwald ripening at room temperatures, which is used to narrow the space and size distribution of nanocrystals [14]. In this respect, it is essential to know the difference between the susceptibility to amorphization of the material of interest in the nanocrystal and bulk phases, to avoid the dose-effect complications and also, from a fundamental point of view, investigate the particular behaviour of a semiconductor crystal confined in an amorphous surrounding. Using a combination of MD computer simulations and *EXAFS* experiments, we now study the crystalline-to-amorphous transition in the elemental bulk and Ge nanocrystal (Ge-*nc*) embedded into amorphous silica (a-SiO_2).

2 Methods

2.1 Computer simulation

By means of the PARCAS molecular dynamics (MD) code [15] we constructed two atomic models of Ge-*nc*'s (spheres 2.4 and 4 nm in diameter) embedded into an *a*-SiO_2 cubic cell with the side length bigger than the diameter of the *nc*. The detailed description of the technique to create a realistic interface between crystalline and amorphous structures is given in [16]. One of the 4 nm as-prepared Ge-*nc*'s is shown in Fig. 1 (a).

In our simulation the Watanabe-Samela potential [17,18] for Si-O mixed systems was applied. The Ge and Ge-Si interatomic interactions were Stillinger-Weber-like potentials modified to give a realistic melting point [19,20]. The Ge-O interaction was obtained by scaling the Si-O potential [17,18] to give a realistic cohesive energy and bond length in GeO_2.

Some details of the simulation of the ion irradiation process can be found in [21]. The high energy ions during the experimental irradiation process pass through the layer with nanocrystals. Hence it is sufficient to consider the modification of this layer caused by the primary self-recoils. In the present work, we simulate dose accumulation as a sequence of atom-mixing cascades initiated by the 0.1 and 1 keV self-recoils, randomly chosen either among nanocrystal atoms (Ge) in an isotropically random direction or among silica atoms (Si or O) in the vicinity of the nanocrystal, but directed only towards it. A newly coming energetic recoil initiates a cascade over the results of the previous one. The dose (in units of energy/atom) was calculated directly from

the kinetic energies of the Ge atoms in the nanocrystal. The statistics for cohesive energy alteration during a long-term irradiation was collected over 5 independent cases of irradiation of the samples with Ge nanocrystals.

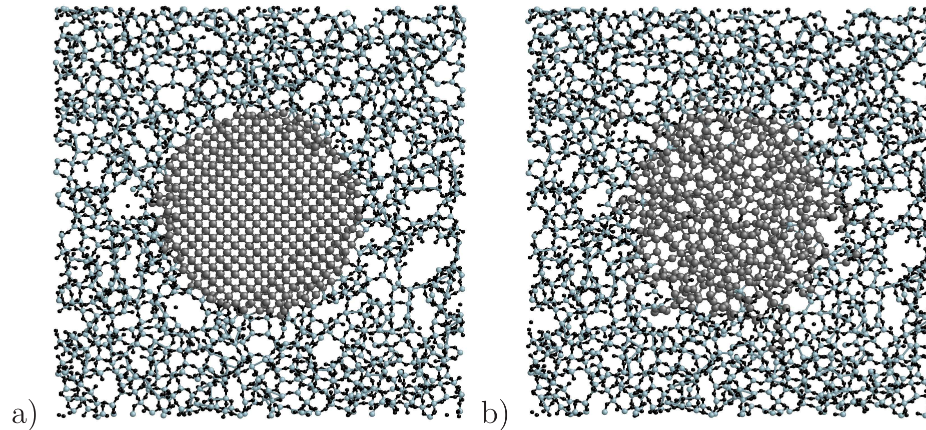

Figure 1. The atomistic model of Ge-*nc*'s (4 nm, larger grey balls in the middle of the cells) embedded into *a*-SiO_2 (smaller grey balls stand for Si and black balls are for O atoms) before (*a*) and after (*b*) high-dose irradiation. The dose effect was simulated as a multiple impact initiated by 100 eV self-recoils.

To obtain a point of comparison, we also carried out simulation of 0.1 keV self-recoil irradiation of an initially perfectly crystalline Ge (*c*-Ge) cell with about 4000 atoms in it. Interestingly, test runs with no pressure control showed that – at least in the currently used potential – when the cell size was kept constant at the equilibrium value for the perfect crystal, the system never amorphized, but obtained a steady state defect concentration fluctuating around roughly 10 %. The systems were then at high pressures around 50 kbar, indicating that a high pressure state can enhance defect recombination. When the cell was relaxed to 0 pressure between the irradiation events, it amorphized fully, as expected (see below).

To analyze the degree of amorphization of the simulated cells, we used the angular structure factor P_{st} analysis method [22] extended to also include both

the first and second-nearest neighbours when forming the list of angles. By comparing the distribution of P_{st} values in perfectly crystalline and quenched fully amorphous pure Ge simulation cells, we found that with this extension it is possible to determine with great certainty whether an atom is in a crystalline or amorphous environment.

Moreover, this approach is well suited for comparison with the *EXAFS* experimental method, as both depend on the degree of order in the local environment of an atom. Thus, the P_{st} analysis enables giving a degree of amorphization in the Ge nanocrystals.

2.2 Experiment

As the first step, we formed the Ge *nc*'s in a 2.0 μm thick SiO_2 layer grown on a (100) Si wafer by wet thermal oxidation. We employed the ion implantation of 2.0 MeV $^{74}Ge^{+1}$ ions with a fluence of 1x10^{17} cm^{-2} and at liquid nitrogen temperature. The formation of the nanocrystals was completed by subsequent thermal annealing at 1060 °C for 1 h under forming gas (N_2 95%, H_2 5%).

Then we irradiated the nc's at liquid nitrogen temperature with 5.0 MeV $^{28}Si^{+3}$ ions over a fluence range of 2x10^{11} to 2x10^{13} cm^{-2}. The energy of such ions when they reach the centre of the Ge distribution was about 2.2 MeV, as given by SRIM2006. The electronic and nuclear energy losses at this energy were 1.730 keV/nm and 0.045 keV/nm in SiO_2 and 1.900 keV/nm and 0.070 keV/nm in Ge, respectively. Additional details on the experimental setup can be found in [23,24].

Comparing the unirradiated and irradiated samples we found no significant

redistribution of Ge in the SiO_2 after the irradiation of the *nc*'s (RBS). Also, we observed that the possible changes in the shape of the spherical particles or their size distribution were negligible for all the irradiation fluences. The maximum of the distribution was at 4.0 nm and the full width at half maximum (FWHM) was 2.0 nm ($\pm$ 5%) (Fig. 2).

We monitored the degree of amorphization of the *nc*'s by analyzing the structural disorder within the Ge *nc*'s through the first shell *EXAFS* Debye-Waller factor, which is an effective measure of the variance of the distribution of distances (or the total disorder). The *EXAFS* measurements were performed at low temperature ($\sim$ 10 K) to minimize the thermal contribution to the total disorder, assumed to be independent of the structural contribution.

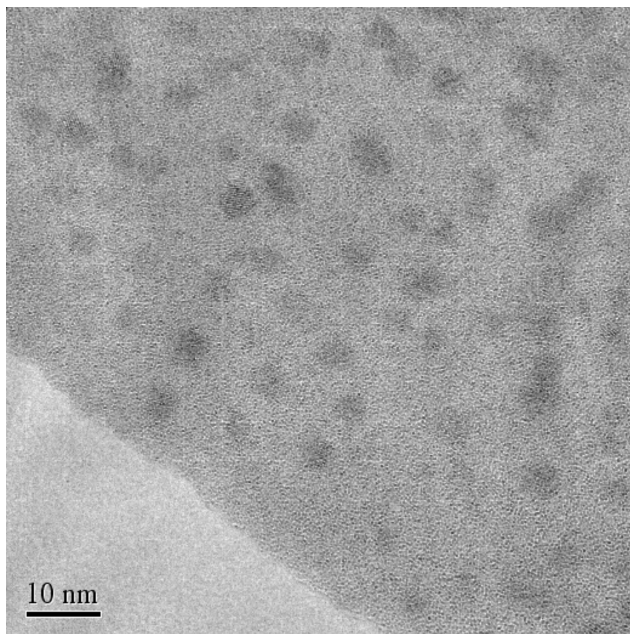

Figure 2. TEM image taken at the depths around the Ge concentration peak for samples annealed at 1060 °C, 1 h.

3 Results and discussion

Fig.1 shows the structures of Ge-nc/SiO_2 with 4 nm Ge-nc before and after amorphization due to ion irradiation. The perfect crystal structure of the Ge nanocrystal (a) appears after irradiation fully disordered, mixing slightly with the interface atoms of silica matrix (b).

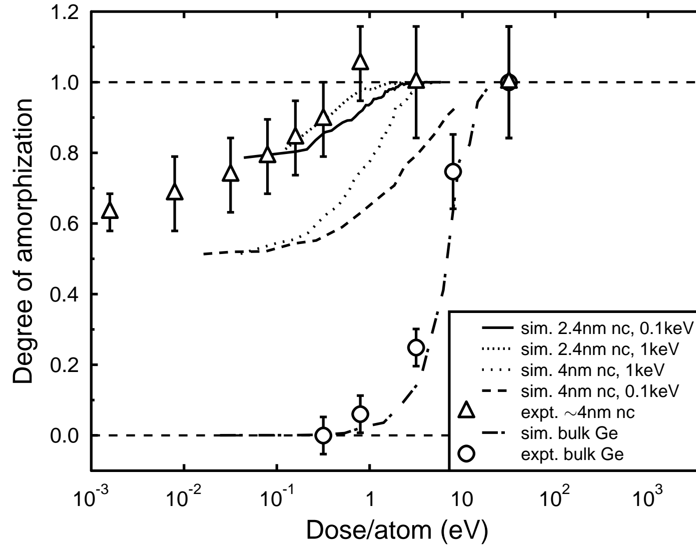

Figure 3. Degree of amorphization versus the irradiation dose for both Ge-nc (4 nm size) and c-Ge.We also show the simulation results for the 2.4 nm nanocrystal for the comparison. Here the experiment is shown as an $EXAFS$ Debye-Waller value and the simulation is presented as a structural factor [22] .The horizontal dash lines indicate the Debye-Waller factors for unirradiated bulk c-Ge and a-Ge. The experimental dose was recalculated to deposited energy per atom using the nuclear deposited energy obtained from SRIM [25]. The statistical uncertainty of the simulated data is $< 2\%$ for the nc simulations and $< 7\%$ for the bulk simulations.

Both simulated P_{st} and experimental $EXAFS$ Debye-Waller factors are shown in Fig. 3 as functions of irradiation dose. The comparison shows a clear agreement between the experimental and simulated results. Despite the fact that while simulating we took into account only the cascades initiated by the primary recoils with the same initial energy, the degree of amorphization with increase of the dose follows very closely the one observed experimentally, especially in case of *c*-Ge. The amorphization curves for the nanocrystals do not agree quite as well, but since the recoil spectra are different and the comparison between EXAFS and structure factor analysis is not direct, it is not at this stage clear what the source of the minor discrepancy is. Most importantly, however, both trends show that it is clear that the evolution with irradiation dose for the *c*-Ge and Ge-*nc* curves are dramatically different. In particular, we observed in the experiment the clear amorphization of Ge-*nc*'s already at the dose 0.8 eV/atom (fluence of 5×10^{13} Si cm^{-2}, cf. Fig. 3), while the bulk *c*-Ge is hardly changed at this dose and started to be amorphized after irradiation with 2×10^{15} Si cm^{-2}. At the same time, the difference in the amorphization doses for both *c*-Ge and Ge-*nc* we estimate as an order of magnitude, which is even greater for the smaller Ge-*nc*'s. The analysis of the interface between Ge-*nc* and *a*-SiO_2 in the MD simulated cell shows the presence of a fair amount of coordination defects ($\sim 15\%$) and stretched bonds.

The average potential energy of atoms in the interface is at least 0.2 eV/atom higher compared to atoms in the rest of the cell (for the same type of atoms). Fig. 3 clearly shows that the *nc* confined in the dielectric matrix is partly amorphized already at the zero dose due to the presence of the interface. The smaller size of the *nc* gives a higher starting point of the amorphization curve. According to an analysis of the spatial distribution of potential energy per

atom, all the disturbance in the structure before ion irradiation is located in the interface area. This is reflected in near-interface atoms being interpreted as amorphous in the structure factor analysis, which strongly indicates that the interface disorder is also the reason that the EXAFS amorphization level starts from a non-zero level. Thereby, we conclude that the stress delivered to a nanocrystal by amorphous surrounding significantly enhances the amorphization of the crystalline structure, which must be undoubtedly taken into account while the ion irradiation is applied for the modification of nanocrystal structures.

4 Conclusions

By combination of MD simulation and *EXAFS* analysis we studied the crystal-to-amorphous transition due to ion irradiation in the Ge-*nc* + *a*-SiO_2 structure. In the present study, we created two atomistic models of Ge-*nc*'s of 2.4 and 4 nm in diameter surrounded by perfectly amorphous SiO_2, which fit the range of the size distribution of nanocrystals formed experimentally. As a result, the *nc* structures showed a higher susceptibility to the amorphization dose compared to bulk *c*-Ge. We explain the lower amorphization dose for the Ge-*nc*'s (more than an order of magnitude) by the presence of the interface area in the *nc*'s, where we observe about 15% of coordination defects. The finite-size effect increases with decreasing size of the *nc*, since the greater part of atoms is involved into the formation of interface.

Acknowledgements

This work was performed within the Finnish Centre of Excellence in Computational Molecular Science (CMS), financed by The Academy of Finland and the University of Helsinki, and also financed by Academy projects OPNA and CONADEP. Grants of computer time from the Center for Scientific Computing in Espoo, Finland, are gratefully acknowledged. We also thank the Australian Synchrotron Research Program, funded by the Commonwealth of Australia, and the Australian Research Council for support.

References

[1] S. Koffela, A. Claverie, G. BenAssayag, and P. Scheiblin, Mater. Res. Soc. Symp. Proc. 9 (2006) 664.

[2] Y. L. Chao, S. Prussin, J. C. S. Woo, and R. Sholz, Appl. Phys. Lett. 87 (2005) 142102, DOI:10.1063/1.2076440.

[3] A. Satta, E. Simoen, T. Clarysse, T. Janssens, A. Benedetti, B. D. Jaeger, M. Meuris, and W. Vandervorst, Appl. Phys. Lett. 87 (2005) 172109, DOI:10.1063/1.2117631.

[4] A. vom Felde, J. Fink, T. Müller-Heinzerling, J. Pflüger, B. Scheerer, and G. Linker, Phys. Rev. Lett. 53 (1984) 922.

[5] K. K. Bourdelle, A. Johansen, and E. Johnson, Nucl. Instr. Meth. Phys. Res. B 118 (1996) 472.

[6] D. Dalacu and L. Martinu, Appl. Phys. Lett. 77 (2000) 4283.

[7] G. Kellermann and A. F. Craievich, Phys. Rev. B 65 (2002) 134204.

[8] H. Rösner, P. Scheer, J. Weissmüller, and G. Wilde, Phil. Mag. Lett. 83 (2003) 511.

[9] A. Singh and A. P. Tsai, Sadhana 28 (2003) 63.

[10] Q. Xu et al., Phys. Rev. Lett. 97 (2006) 155701.

[11] J. A. Pakarinen, M. Backman, F. Djurabekova, and K. Nordlund, Phys. Rev. Lett. (2007), submitted for publication.

[12] B. Johannessen, P. Kluth, D. J. Llewellyn, G. J. Foran, D. J. Cookson, and M. C. Ridgway, Appl. Phys. Lett. 90 (2007) 073119.

[13] L. Pavesi and G. Guillot, *Optical Interconnects: The silicon approach*, chapter 2.Optical gain and the quest for a silicon injection laser, pp. 17–32, Springer, Berlin, 2006.

[14] K. H. Heinig, B. Schmidt, M. Strobel, and H. Bernas, Mater. Res. Soc. Symp. Proc. 650 (2001) R9.6.1/O14.6.1.

[15] K. Nordlund, PARCAS computer code (2007).

[16] F. Djurabekova and K. Nordlund, Phys. Rev. B 77 (2008) 115325, also selected to Virtual Journal of Nanoscale Science & Technology Vol. 17 Issue 13 (2008).

[17] T. Watanabe, D. Yamasaki, K. Tatsumura, and I. Ohdomari, Appl. Surf. Sci. 234 (2004) 207.

[18] J. Samela, K. Nordlund, V. N. Popok, and E. E. B. Campbell, Phys. Rev. B 77 (2008) 075309.

[19] K. Ding and H. C. Andersen, Phys. Rev. B 34 (1986) 6987.

[20] K. Nordlund, M. Ghaly, R. S. Averback, M. Caturla, T. Diaz de la Rubia, and J. Tarus, Phys. Rev. B 57 (1998) 7556.

[21] F. Djurabekova, M. Backman, and K. Nordlund, Nucl. Inst. and Meth. in Phys. Res., B 266 (2008) 2683.

[22] K. Nordlund and R. S. Averback, Phys. Rev. B 56 (1997) 2421.

[23] M. C. Ridgway, G. de M. Azevedo, R. G. Elliman, C. J. Glover, D. J. Llewellyn, R. Miller, W. Wesch, G. J. Foran, J. Hansen, and A. Nylandsted-Larsen, Phys.Rev. B 71 (2005) 094107.

[24] L. L. Araujo, R. Giulian, B. Johannessen, D. J. Llewellyn, P. Kluth, G. D. M. Azevedo, D. J. Cookson, G. J. Foran, and M. C. Ridgway, Nucl. Inst. and Meth. in Phys. Res.B 266 (2008) 3153.

[25] J. F. Ziegler, SRIM-2008 software package, available online at *http://www.srim.org*.